EEG-based methods to characterize memorised visual space*

Mauro Nascimben[1,2], Thomas Zoëga Ramsøy[1], and Luis Emilio Bruni[2]

[1] Neurons Inc, Taastrup, Denmark
https://neuronsinc.com/
[2] Augmented Cognition Laboratory, Aalborg University Copenhagen, Denmark
https://augcog.aau.dk/

Abstract. One second of memory maintenance was evaluated to determine EEG metrics ability to track memory load and its variations connected with the lateral presentation of objects in the visual hemi-field. An initial approach focused on features gathered from the N2pc time series to detect the memory load using ensemble learners.Conversely, the secondary approach employed a regularised support vector classifier to predict the area of N2pc event-related components, identifying 6 levels of memory load and stimulus location.

Keywords: Visual working memory · Memory load · Retention period.

1 Introduction

1.1 Visual working memory and cognitive load

Visual working memory (i.e. VWM) supports high cognitive functions providing temporary storage for retained information from one fixation to the next. The visual features primarily maintained in mind are position, shape, color and texture of the objects in space commonly referred an object's attributes above the perceptive threshold [1]. The number of items stored in memory is rather related to the concept of capacity [2] and limited to 3-4 multi-attribute objects [3] depending on subjective performance and task characteristics (for example, encoding time [4]). Multitasking impacts the number of memory items that can be maintained and the amount of cognitive resources expended [5]. Indeed, working memory not only includes maintenance of information, but also information processing during encoding time of filtering irrelevant stimuli (distractor avoidance) [6]. Such multiprocessing is commonly termed the cognitive load. The time-based resource-sharing model [7] aims to theorize the relationship between cognitive load and memory performance by identifying four major mental stages: encoding, filtering distractors, recall, and refreshing-the last of

* This project has received funding from the European Union's Horizon 2020 research and innovation programme under the Marie Skłodowska-Curie Grant Agreement No 813234.

which redirects attention to restore dwindled items into memory. While learning during a classroom lesson, students need to manage mental resources in order to continuously acquire incoming information and effectively manipulate it. When information to be held oversteps working memory capacity, cognitive overload is experienced [8]. Naturally, what happens during the classroom experience could be extended to other real-world scenarios. In multimedia, visual and audio streams are processed in humans by two separate brain circuitry both with limited working memory capacity, thus active processing of both streams could exceed the audience's available cognitive capacity. This is not only due to the essential processing of audio or video materials, but also caused by environmental disturbances or confusion in the presentation of multimedial contents [9].

1.2 Neurophysiologic correlates of VWM

In literature three components are commonly attributed to VWM. Two of them are event-related potentials (i.e. ERP), one called controlateral delayed activity (i.e. CDA) and the other N2pc. The third correlate of VWM is an induced modification over occipito-parietal electrodes in alpha band, where one observes a decreased alpha power when an individual retains information in memory.

Lateralization of stimuli in the visual hemifield During VWM experimental evaluation, an event related potential called controlateral delayed activity (i.e. CDA) [10] was identified on posterior-occipital areas usually interpreted as a neural marker of the number of items stored in memory. Moreover, CDA polarity changes depending on the position of the elements memorized in the visual space. Despite an alternative hypothesis claiming a relationship between the CDA wave and spatial attention [11], current findings confirm the relation between CDA and memory capacity [12], [13]. In subjects with lower memory capacity, distractors presented alongside targets in the visual field increased CDA amplitudes compared to individuals with better capacity [14].

Deployment of visual attention ERPs can track shifts of attention to the targets: the N2pc wave specifically reflects the attention towards an object [15], [16]. This wave appears between 180 and 300ms (usually peaking at a latency of 250ms) with enhanced amplitude over the posterior-occipital electrodes controlateral to the visual targets present in the visual field. In [17], the authors describe a relationship between N2pc and the processing load: visuo-spatial configurations that require more time to be evaluated demand a sustained involvement of attention reflected by higher N2pc amplitudes. N2pc appears not only as a metric of attention for targets in the extra-personal space, but mreover N2pc amplitudes are modulated during memory retention to weigh information according to its relevance [18].

Relation between alpha oscillations and memory functions Alpha oscillatory activity is suppressed during memory encoding likely due to visual processing, whilst alpha is enhanced in the course of memory maintenance to prevent competition for resource allocation with incoming visual stimuli [19]. Throughout memory retention alpha waves could phase-couple with other frequencies like beta or gamma in organized neural networks [21]. Patterns of alpha desynchronization during encoding and synchronization for memory maintenance appear in form of induced power changes that are not time-locked to stimuli.

2 Methods

Experimental paradigm Data was released by authors of the paper [22] in pre-processed format. The present study solely retained the healthy subjects, originally denoted as the comparison group. Participants were 27 college students (11 females) with an average age of 22 years. The experimental paradigm was adapted from [23] with an initial presentation of an array of geometrical shapes succeeded by a memory maintenance period of one second. Prior to each trial, an arrow appearing at the center of the screen informed the subjects which visual hemi-field they should memorize (left "L" or right "R"), while during each trial an array of colored shapes was displayed for 200ms. Subsequently, the object array disappeared, requiring the subjects to store the visual information into their working memory. Following a memory retention period of one second, participants would then be tasked with deciding whether the new object array matched the one presented prior. Half of the trials had one color of a shape changed in the attended side. Three types of object arrays were tested: "low memory load" (i.e. "L") with only 2 squares to be memorised, "high memory load" (i.e. "H") when 4 squares were to be memorised or "distractors" (i.e. "D") with two circles that should be ignored (Fig. 1).

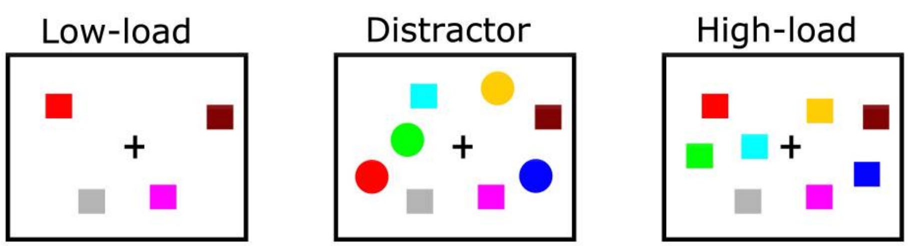

Fig. 1. Experimental stimuli were 2 types of objects (squares and circles) in 10 randomly selected colors (supra-threshold perceptive features) [22]

Pre-processing of neural signals EEG was recorded with a high-density cap of 128 electrodes (Hydrocel Geodesic sensor net) and sampled at 500 Hz. Epochs were 104 for each experimental condition, and those with artifacts were rejected. Further pre-processing steps included filtering (0.05–30 Hz) and re-referencing in common average mode. Epoch length of the memory retention period was 1 second preceded by 0.4s of baseline. For each subject, extra-cephalic electrodes (lower line of the Geodesic cap) were discarded (109 channels kept), and single trial EEG signals had their voltages normalized with z-score procedure (using baseline mean and standard deviation in range -200 to 0ms): z-score standardization on subjective baseline allows one to model a user-independent approach. Procedures involved employed the MNE-python library [25].

Outliers detection Outlier detection is an important preliminary step to identify subjects that the model is unable to generalise, deviating significantly from the rest of the data. Multidimensional scaling reduces dimension of the data by representing the proximity (or similarity) matrix between individuals as a lower dimensional space [24]. The proximity matrix is a configuration of points in Euclidean space such that the inter-point distances approximate the subjective data. In (Fig. 2) dashed lines represent the squared Mahalanobis distances

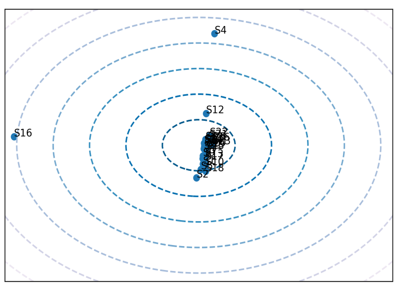

Fig. 2. All subjects in all conditions

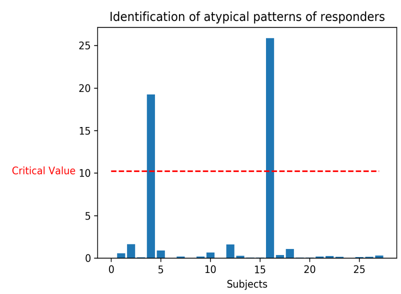

Fig. 3. Outliers critical threshold

of the empirical covariance matrix shown as a visual indicator of adjacency between points. The inclusion criteria implemented a mathematical approach to cut-off outliers by identifying a critical threshold based on the approximated F distribution [26] (Fig. 3). Based on the critical threshold, subjects 4 and 16 were excluded from further analysis.

3 Results

Initially, a total of 5956 signals were further normalized with L2-norm and pair-wise comparisons between conditions obtained with t-test analysis for each channel with significance threshold adjusted by Bonferroni correction. This statistical test was applied to identify a group of electrodes with significant changes between conditions. Indeed in Fig. 4, one observes a high number of differing pair-wise comparisons between 192 and 268 ms. Additionally, an analysis using cluster permutation F-test was conducted in the same data to highlight time frames of relevant activity differing between stimuli, as in [27]. For example, electrode E90 in Fig. 5 illustrates the cluster of significant activity corresponding to N2pc time range (highlighted in orange, p <0.05). Crossing the results of both statistical

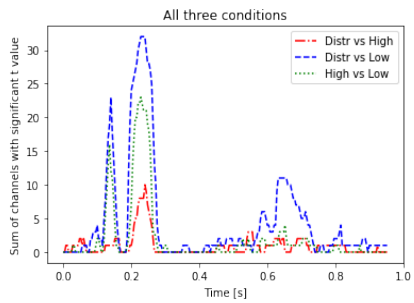

Fig. 4. T-test on all sensor data

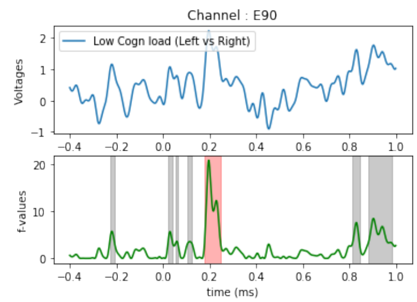

Fig. 5. Permutation test on each sensor

methodologies we obtained a group of electrodes and a time-frame with brain activity relevant to distingush between conditions: mainly posterior-occipital channels during N2pc time course (Fig. 6).

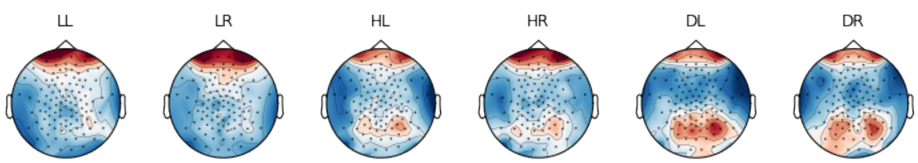

Fig. 6. Topographic plots at 240ms (color scale blue to red from -2.65 to 3.56 μV)

3.1 Cognitive load prediction

Analysis focused on prediction of three cognitive states using the time series extracted from the N2pc wave on parieto-occipital electrodes.Number of trials were equalized randomly under-sampling the most represented classes. From the time course of the N2pc, 794 features were extracted using 63 characterization methods [28]. Redundant features were eliminated by the statistical approach presented in [29], and divided in train and test sets with a 80% and 20% split. Test set accuracy is reported in Table 1 comparing two classification methods each with hyperparameters tuned by a combination of cross-validated (5 folds with stratification) randomized and grid search on train set.The chance level was calculated as 51.96% according to the binomial cumulative distribution as in [30] with a significance threshold set at p=0.05.

Ensemble method	Distr vs High	Distr vs Low	High vs Low
Random Forest	72%	73%	69%
Gradient Boosting	72%	71%	71%

Table 1. Cognitive load prediction one-vs-one

3.2 Prediction of Cognitive load and stimuli location

In this investigation six classes were inspected: three cognitive load levels ("L", "H", "D") by two different locations of the stimuli in the visual hemi-field ("L" or "R"). In Fig. 7, the global field power (i.e. GFP) from all electrodes is used to identify a time window enclosing the N2pc wave. Indeed, permutation t-test with pair-wise comparisons (significance adjusted by the "false discovery rate") between conditions identified two clusters of significant electrodes, one over the parieto-occipital, and one over the fronto-central areas (Fig. 8). Area of the N2pc

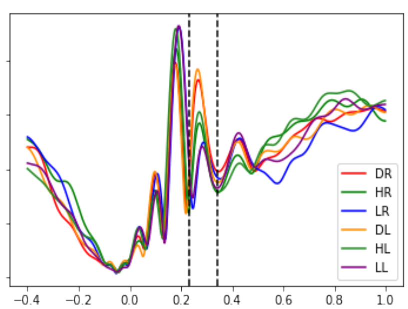

Fig. 7. GFP of the experimental conditions

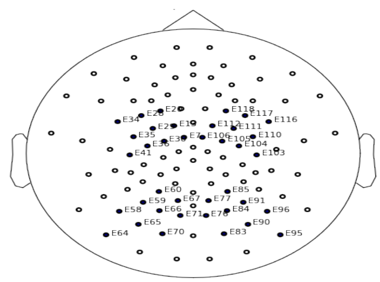

Fig. 8. 38 identified electrodes

from each single trial over the identified electrodes was used as feature for an SVM classifier. Classes were balanced by randomly under-sampling trials of the most represented labels (5346 trials used as observations). A support vector machines (i.e. svm) model with radial basis function (i.e. rbf) as kernel was selected as classifier and data was divided in the aforementioned 80-20 split. Kernel and regularization parameters were optimized by grid search with cross-validation (5 stratified folds and validation size 20%) and classification methodology one-versus-rest. Outcomes against a dummy svm-rbf classifier are shown in Table 2 using F1 score as metric (last two columns are weighted-average F1 and micro-F1 scores). Statistical chance level calculated as in [30] was 17.5% (at p=0.05).

4 Conclusions

Two procedures are presented to distinguish between the levels of cognitive resources deployed during retention period of the visual working memory: the first

	DL	HL	LL	DR	HR	LR	w-F1	Micro
SVM	0.657	0.642	0.538	0.603	0.325	0.570	0.552	0.560
Dummy	0.126	0.150	0.168	0.163	0.158	0.152	0.153	0.153

Table 2. Prediction of cognitive load and stimulus location

based on features extracted from the N2pc time series whereas the second involves using the area of N2pc component. The latter offers a promising technique for categorizing not only the memory load, but also the location of the stimuli in the visual hemi-field (overall accuracy +38.5% above chance level).

References

1. Patel, S. S., Bedell, H. E., Tsang, D. K., Ukwade, M. T. (2009). Relationship between threshold and suprathreshold perception of position and stereoscopic depth. JOSA A, 26(4), 847-861.
2. Luck, S. J., Vogel, E. K. (2013). Visual working memory capacity: from psychophysics and neurobiology to individual differences. Trends in cognitive sciences, 17(8), 391-400.
3. Vogel, E. K., Awh, E. (2008). How to exploit diversity for scientific gain: Using individual differences to constrain cognitive theory. Current Directions in Psychological Science, 17(2), 171-176.
4. Barrouillet, P., Bernardin, S., Portrat, S., Vergauwe, E., Camos, V. (2007). Time and cognitive load in working memory. Journal of Experimental Psychology: Learning, Memory, and Cognition, 33(3), 570.
5. Zheng, Z. (2018). Cognitive Load Measurement and Application. Routledge: New York, NY, USA.
6. Lavie, N., De Fockert, J. (2005). The role of working memory in attentional capture. Psychonomic bulletin review, 12(4), 669-674.
7. Oberauer, K., Lewandowsky, S. (2011). Modeling working memory: A computational implementation of the Time-Based Resource-Sharing theory. Psychonomic bulletin review, 18(1), 10-45.
8. Puma, S., Matton, N., Paubel, P. V., Tricot, A. (2018). Cognitive load theory and time considerations: Using the time-based resource sharing model. Educational Psychology Review, 30(3), 1199-1214.
9. Mayer, R. E., Moreno, R. (2003). Nine ways to reduce cognitive load in multimedia learning. Educational psychologist, 38(1), 43-52.
10. Vogel, E. K., Machizawa, M. G. (2004). Neural activity predicts individual differences in visual working memory capacity. Nature, 428(6984), 748-751.
11. Berggren, N., Eimer, M. (2016). Does contralateral delay activity reflect working memory storage or the current focus of spatial attention within visual working memory?. Journal of Cognitive Neuroscience, 28(12), 2003-2020.
12. Pomper, U., Ditye, T., Ansorge, U. (2019). Contralateral delay activity during temporal order memory. Neuropsychologia, 129, 104-116.
13. Feldmann-Wüstefeld, T., Vogel, E. K., Awh, E. (2018). Contralateral delay activity indexes working memory storage, not the current focus of spatial attention. Journal of cognitive neuroscience, 30(8), 1185-1196.

14. Vogel, E. K., McCollough, A. W., Machizawa, M. G. (2005). Neural measures reveal individual differences in controlling access to working memory. Nature, 438(7067), 500-503.
15. Eimer, M. (1996). The N2pc component as an indicator of attentional selectivity. Electroencephalography and clinical neurophysiology, 99(3), 225-234.
16. Hickey, C., McDonald, J. J., Theeuwes, J. (2006). Electrophysiological evidence of the capture of visual attention. Journal of cognitive neuroscience, 18(4), 604-613.
17. Maheux, M., Jolicœur, P. (2017). Differential engagement of attention and visual working memory in the representation and evaluation of the number of relevant targets and their spatial relations: evidence from the N2pc and SPCN. Biological psychology, 125, 28-35.
18. Heuer, A., Schubö, A. (2016). The focus of attention in visual working memory: Protection of focused representations and its individual variation. PloS one, 11(4).
19. Wianda, E., Ross, B. (2019). The roles of alpha oscillation in working memory retention. Brain and behavior, 9(4), e01263.
20. Baars, B. J., Gage, N. M. (2010). Cognition, brain, and consciousness: Introduction to cognitive neuroscience. Academic Press.
21. Palva, S., Palva, J. M. (2007). New vistas for -frequency band oscillations. Trends in neurosciences, 30(4), 150-158.
22. Gu, C., Liu, Z. X., Tannock, R., Woltering, S. (2018). Neural processing of working memory in adults with ADHD in a visuospatial change detection task with distractors. PeerJ, 6, e5601.
23. Vogel, E. K., McCollough, A. W., Machizawa, M. G. (2005). Neural measures reveal individual differences in controlling access to working memory. Nature, 438(7067), 500-503.
24. Groenen, P. J., Heiser, W. J. (1996). The tunneling method for global optimization in multidimensional scaling. Psychometrika, 61(3), 529-550.
25. Gramfort, A., Luessi, M., Larson, E., Engemann, D. A., Strohmeier, D., Brodbeck, C., ... Hämäläinen, M. (2013). MEG and EEG data analysis with MNE-Python. Frontiers in neuroscience, 7, 267.
26. Riani, M., Atkinson, A. C., Cerioli, A. (2009). Finding an unknown number of multivariate outliers. Journal of the Royal Statistical Society: series B (statistical methodology), 71(2), 447-466.
27. Maris, E., Oostenveld, R. (2007). Nonparametric statistical testing of EEG-and MEG-data. Journal of neuroscience methods, 164(1), 177-190
28. Christ, M., Braun, N., Neuffer, J., Kempa-Liehr, A. W. (2018). Time series feature extraction on basis of scalable hypothesis tests (tsfresh–a python package). Neurocomputing, 307, 72-77.
29. Christ, M., Kempa-Liehr, A. W., Feindt, M. (2016). Distributed and parallel time series feature extraction for industrial big data applications. arXiv preprint arXiv:1610.07717.
30. Combrisson, E., Jerbi, K. (2015). Exceeding chance level by chance: The caveat of theoretical chance levels in brain signal classification and statistical assessment of decoding accuracy. Journal of neuroscience methods, 250, 126-136.